

The Role of Niobium as Microalloy in Electrical Sheet

Klaus Hulka, Constantin Vlad and Ana Doniga

The processing route of grain oriented electrical sheet was simulated by laboratory trials. Besides MnS, the effect of AlN and NbC as an inhibitor phase in 3 % silicon steel was also investigated. In the hot strip material the niobium microalloyed steel showed the highest volume fraction of the $\{110\}\langle 001 \rangle$ Goss texture at 0.3 to 0.4 mm below the surface. This superiority was maintained after cold rolling and annealing after both, one step or two step cold reduction schedules. A volume fraction of the Goss texture of more than 80 % is typical for this steel concept. It can be explained by the solubility product of NbC, which guarantees grain size control during the primary recrystallization processes and allows the Goss texture component to grow during secondary recrystallization, which usually follows a steel decarburization. Consistent with the highest volume fraction of Goss texture, the core losses are lowest in the sheet using NbC as an inhibitor phase.

Niob als Mikrolegierungselement in Elektroblech. In Laborversuchen wurde der Herstellungsprozeß von Elektroblech simuliert. Neben MnS wurden auch AlN und NbC als Steuerphasen in 3% Siliziumstählen geprüft. Schon im Warmbandmaterial weist der niobmikrolegierte Stahl etwa 0.3 bis 0.4 mm unter der Oberfläche den höchsten Wert der $\{110\}\langle 001 \rangle$ Goss Textur auf. Unabhängig davon, ob ein Einstufen- oder Zweistufen-Kaltwalzprozeß durchgeführt wurde, zeigte diese Legierungsvariante immer die höchsten Volumenanteile von Gosstextur, und mehr als 80 % dieser Orientierung ist typisch für geglühtes Elektroblech, das niobmikrolegiert ist. Man kann dies mit Hilfe des Löslichkeitsprodukts von NbC erklären: bei den typischen Glühtemperaturen der primären Rekristallisation verhindert Niobkarbid das Kornwachstum, erlaubt aber während der sekundären Rekristallisation, die auf einen Entkohlungsprozeß folgt, ein Wachsen der Gosstextur. In Übereinstimmung mit den höchsten Volumenanteilen von Gosstextur weist das Elektroblech mit NbC als Steuerphase die niedrigsten Wattverluste auf.

Progress in the electrical and electronic industries during the last century can be correlated with the improvement in magnetic materials and advances in their technology; e.g. the reduction of energy losses in magnetic materials of generators, motors and transformers.

It has been demonstrated that a relatively small core loss is experienced in silicon steel sheet, which is the most common soft magnetic material used in the electrical industry [1, 2]. The core loss is influenced by several factors, from which the eddy-current and hysteresis losses can be distinguished. The eddy-current losses consist of intrinsic eddy-current losses, which depend on the silicon content and the sheet thickness, and the anomalous eddy-current losses which depend on the domain width configuration. Hysteresis losses, on the other hand, are affected by grain orientation, cleanliness, and internal stresses.

The development of a favourable crystallographic orientation is another feature of electrical sheet steel. The cube-on-edge $\{110\}\langle 001 \rangle$ orientation or Goss texture [3] is the most prominent one and is mainly used for transformers operating at lower induction. The technologies to produce grain oriented electrical sheet have been developed in the 1950's and early 1960's, at a time when niobium was not abundantly available. Therefore in this study the effect of niobium microalloying on texture development and the resulting magnetic properties has been studied.

Alloy design and processing of grain oriented silicon steel

In the making of grain oriented silicon steel, high requirements in the cleanliness are a prerequisite. This is especially problematic with aluminium containing steels, which naturally exhibit alumina inclusions and bear the danger of internal oxidation [4].

Pure iron with more than 2.15% Si is completely ferritic, which is beneficial to control the crystallographic texture as no transformation stresses occur. However, silicon steel with higher content of carbon (austenite stabilizing element) may exhibit a certain austenite level at a temperature of about 1100 °C owing to the occurrence of the $\alpha+\gamma$ two phase region [5]. Thus, carbon levels greater than 0.05% should be avoided. In addition, a high hot rolling temperature aids to complete hot deformation in the ferrite region. Furthermore, the manganese content is kept at a relatively low level of 0.06 to 0.08% in order to promote a sluggish primary recrystallization by forming Mn-O-S dipole clusters [6].

The processing of grain oriented silicon steel is rather complex and a typical processing route following steel-making and continuous casting is given in **Table 1**. Various cold rolling steps and annealing procedures are needed to maximize the Goss texture component. The characteristic heat treatment is a high temperature anneal, representing the most important industrial application of secondary recrystallization. It depends upon the ability of a few grain boundaries to break away from pinning points [6]. One achieves a strong Goss texture in processing silicon steel when grain growth is retarded during the preceding process of primary recrystallization, which can be obtained by introducing particles being able to pin the grain boundaries. Consequently, a high volume fraction and homogeneous distribution of particles, called 'inhibitor phase', is aimed for. One means to achieve the desired particle distribution is by their dissolution during slab soaking and re-precipitation during hot rolling. There are numerous compounds that can serve this purpose, the most prominent being MnS and AlN [7,8]. However, in order to allow secondary recrystallization to occur, these particles have to be removed (dissolved again) or at least have to coarsen remarkably. Since such

particles would also restrain domain wall motion and thus causing higher core losses, their removal has a double positive effect.

Table 1: Processing route for grain oriented silicon steel sheet

- Slab reheating to a temperature of about 1350 °C
- Hot strip rolling and coiling
- Hot band annealing 'normalizing' (optional)
- Pickling
- 1st cold rolling – Sendzimir mill
- Primary recrystallisation - Continuous annealing line
- 2nd cold rolling - Sendzimir mill
- Decarburisation and 2nd primary recrystallisation - continuous annealing line
- Coating – separator line
- Secondary recrystallisation - high temperature batch annealing in dry hydrogen
- Thermal flattening - continuous annealing line
- Isolation - coating line
- Shearing and slitting – finishing line

Solubility products

A first classification of the potential of an inhibitor phase is possible by its solubility product. By comparing the solubility products of various nitrides in ferrite, such as ZrN [9], TiN [9], BN [10], AlN [11], NbN [9] and VN [12] with niobium carbide NbC [9] - since niobium forms carbonitrides - and MnS [13], the following ranking is observed:

$$\log [(\%Zr) \times (\%N)] = -18160/T + 5.24 \quad (1)$$

$$\log [(\%Ti) \times (\%N)] = -17640/T + 6.17 \quad (2)$$

$$\log [(\%B) \times (\%N)] = -13560/T + 4.53 \quad (3)$$

$$\log [(\%Al) \times (\%N)] = -9595/T + 2.65 \quad (4)$$

$$\log [(\%Nb) \times (\%N)] = -10650/T + 3.87 \quad (5)$$

$$\log [(\%V) \times (\%N)] = -8120/T + 2.48 \quad (6)$$

$$\log [(\%Nb) \times (\%C)] = -10990/T + 4.62 \quad (7)$$

$$\log [(\%Mn) \times (\%S)] = -8400/T + 2.77 \quad (8)$$

Thus suggesting that niobiumcarbonitrides are a promising compound.

Compared to the solubility product in pure iron, the solubility in 3% silicon-iron is remarkably reduced. The solubility products for common inhibitor phases such as BN [14], AlN [15] and MnS [16] in 3% silicon-iron are given in **Figure 1**. They follow the equations:

$$\log [(\%B) \times (\%N)] = -19560/T + 7.75 \quad (9)$$

$$\log [(\%Al) \times (\%N)] = -11900/T + 3.56 \quad (10)$$

$$\log [(\%Mn) \times (\%S)] = -14855/T + 6.82 \quad (11)$$

Assuming that the niobium compounds respond in a similar mode to the silicon addition, the solubility products for the niobium nitride and niobium carbide in 3% silicon-iron alloys follow the equations:

$$\log [(\%Nb) \times (\%N)] = -13700/T + 5.20 \quad (12)$$

$$\log [(\%Nb) \times (\%C)] = -14500/T + 6.25 \quad (13)$$

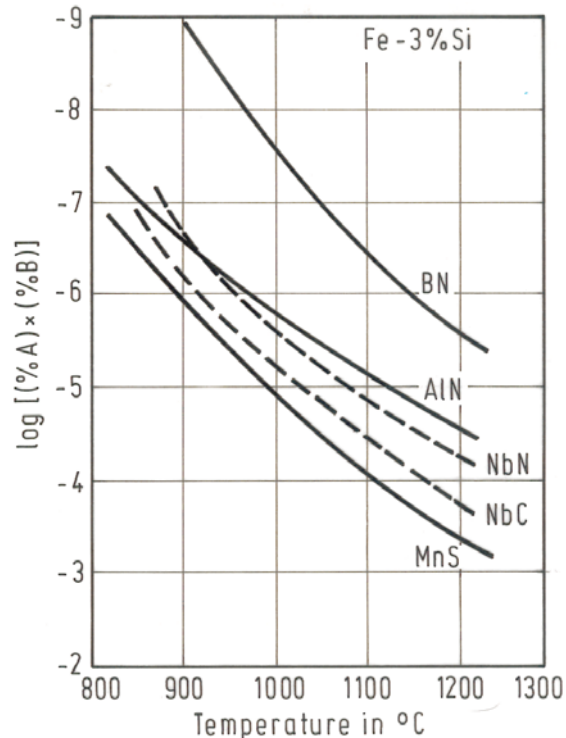


Figure 1: Solubility products of various compounds in 3% Si iron

Experimental materials and procedures

Within this study, three steels of different chemical composition have been investigated, as highlighted in **Table 2**.

Steel A originated from a commercially produced continuous cast slab, typical for the silicon steel produced in Romania according to the know-how from US Steel [17]. The inhibitor phase in this steel is MnS.

Steels B and C are laboratory melts of about 50kg produced in a vacuum induction furnace with a pressure of 8×10^{-2} Torr, where either AlN or Nb(C,N) have been selected as inhibitor phase in addition to MnS. The bulk chemical composition of the laboratory heats was similar to steel A of industrial production.

The experimental material was machined to 125 x 125 x 375mm plates. After reheating to 1350°C for 1.5 hours it was forged in two steps to plates of 40 x 120 x 305mm and 7 x 100 x 300mm respectively.

Table 2: Chemical Composition of Investigated Steels

Steel	% C	% Si	% Mn	% P	% S	% Al _{tot} / %Al _{sol}	% Nb	% O	% N
A ('MnS')	0.029	3.04	0.07	0.009	0.023	0.012	none	0.0076	0.0062
B ('AlN')	0.04	3.02	0.07	0.013	0.023	0.07/0.032	none	0.0078	0.0065
C ('NbCN')	0.04	3.04	0.08	0.009	0.017	0.002	0.09	0.0073	0.0067

During forging the temperature never dropped below 950°C. After cooling to room temperature, with a cooling rate of 2.5°C/s the forged plates were sliced longitudinally and sheared to samples of 7 x 50 x 150mm for further hot rolling. The hot rolling to plates of 2 x 50 x 150mm was carried on a laboratory duo mill, comprising working rolls of 135mm diameter and a rolling force of 200kN. The finish rolling temperature was varied from 1200°C to 900°C and two different cooling rates (air cooling and warm water quench of 100°C) were applied.

In order to check the influence of an annealing treatment of the hot band ('normalizing'), the warm water quenched samples with a finish rolling temperature of 1000°C were annealed at 950°C for 6 to 9 minutes, followed by air-cooling.

The hot rolled plate samples were then cold rolled using two different rolling regimes:

1. In the two stage cold rolling route with an intermediate recrystallization treatment the first deformation step reduced the samples thickness from 2 to 0.7mm: The following intermediate annealing for primary recrystallization used annealing temperatures of 800°C, 920°C or 1050°C respectively and ten different holding times between 5 seconds and 1.5 hours. These samples were sheared to 0.7 x 30 x 75mm and cold rolled from 0.7 to 0.35mm in a second step. Next the samples were decarburized in an H₂ atmosphere at 880°C for a period of 30 minutes, followed immediately by a high temperature anneal for secondary recrystallization at 900°C, 1000°C or 1150°C respectively using three different holding periods of 2, 4 or 6 hours. Even the highest of these temperatures was below the temperature of complete dissolution of the inhibitor phase, calculated according to the equations 10 to 13, which is 1265°C for MnS in steel A 1370°C for AlN in steel B and 1265 or 1352°C for NbC or NbN in steel C. By this procedure, the carbon content in the final 'transformer sheet' was reduced by one order of magnitude compared to the original level, as shown in **Table 3**, and is similar to that of industrial production.

Table 3: Carbon content after decarburization in H₂ atmosphere

Steel	% C
A ('MnS')	0.003
B ('AlN')	0.004
C ('NbC,N')	0.004

In order to determine the influence of the degree of cold rolling reduction, several 0.7mm samples, annealed for 5 minutes at 920°C, were subjected to cold reductions of 40%, 56% or 64%, besides the already described 50%, followed by the described annealing cycle with the final secondary recrystallization at 1150°C for 6 hours.

2. Sheet with the same final thickness of 0.35mm was produced via a single stage cold rolling process. For this study the 7mm plate was hot rolled into samples of 1.7, 2.3 and 3.15mm, respectively, thus providing degrees of cold deformation varying from about 80, via 85 to 90%. For all these samples the secondary recrystallization was also carried out at 1150 °C for 6 hours.

The investigation covered the identification of inclusions as well as the development of the microstructure and the crystallographic texture during the whole processing route. The texture was determined by a reflection method [18] and the volume fractions of the various texture components by an inverse pole figure method [19]. Furthermore, torque measurements were used to confirm these findings. The core losses of the 'transformer sheets' from the laboratory studies were determined for inductions of 0.5, 1.0 and 1.5 Tesla using single strip samples of 30mm width and 180mm length [20] and compared with data from industrial production.

Results and Discussions

Hot rolled samples. All specimens showed a rather high amount of silicate inclusions, often in the form of stringers. Furthermore, steel A contained also elongated manganese sulphides and the two laboratory heats B and C exhibited complex globular inclusions, identified as (Ca, Al, Mn) oxi-sulfides. Besides these inclusions, which had a size of a few microns, fine particles of < 100 nm were also found. These particles were identified by X-ray diffractometry as MnS in steel A, AlN in steel B and both, NbC and NbN, in steel C.

The microstructure of the hot band is shown by one example in **Figure 2**. As already known from the literature [21], three distinct layers were present in all steels: surface-near equi-axed polygonal ferrite grains were observed, indicating complete recrystallization. At a certain distance from the surface the polygonal ferrite grains were more elongated, indicating that recovery or in-situ recrystallization was the dominant softening mechanism, and towards the center of the material a non-recrystallized, deformed microstructure was observed.

Furthermore, the crystallographic texture varied over the cross section of the hot band. **Figure 3** shows that the volume fraction of the rather stable {110}<001> Goss texture exhibited a maximum at a distance of around 0.3mm from the surface, which correlates to the elongated polygonal ferrite grains. The highest value of Goss texture was obtained in the niobium microalloyed steel, followed by the sample relying on AlN technology. At this position the texture component {111}<112> increased to levels of around 28%. Surface near the texture component {110}<111> became dominant, while towards the centre region the cube texture {100}<110> steadily increased from 6 to 8

volume percent: The texture components $\{111\}\langle uvw \rangle$ however are rather equal in all positions [22].

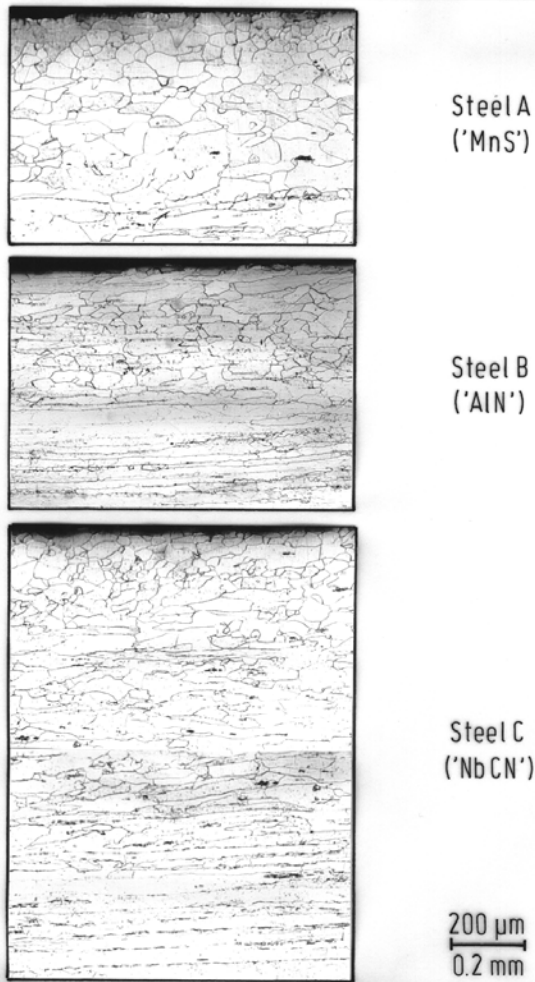


Figure 2: Microstructure surface-near of hot rolled samples (FRT = 900 °C)

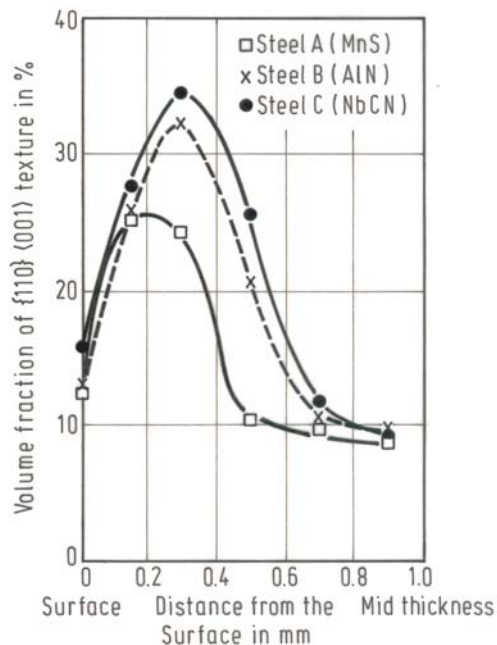


Figure 3: Distribution of Goss texture over the thickness of hot rolled samples (FRT = 900 °C)

The severity of Goss texture in the hot rolled samples also depended on the processing conditions. **Figure 4** shows, that a finish rolling temperature of 1000 °C was most favourable to achieve a high amount of the $\{110\}\langle 001 \rangle$ orientation, especially when the higher cooling rate was applied. The observed reduction in the volume fraction of Goss texture with higher finish rolling temperatures than 1000 °C is according to expectations. The lower volume fraction of Goss texture obtained after finish rolling at 900 °C is probably caused by a certain transformation from α into γ -iron at this temperature.

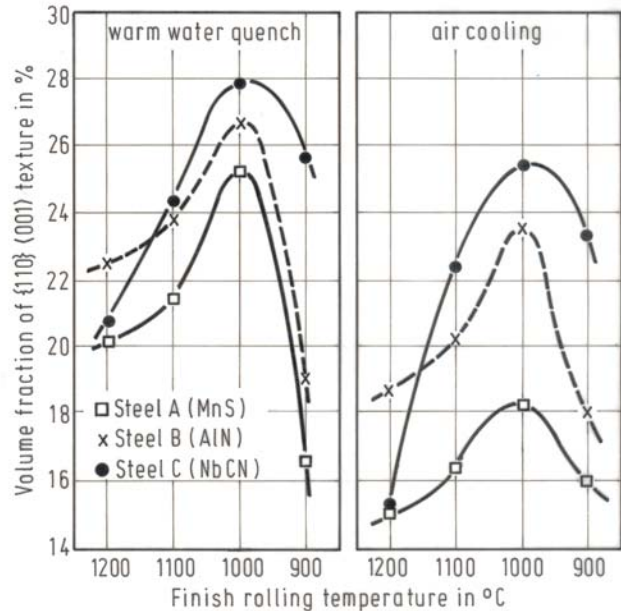


Figure 4: Influence of hot rolling and cooling conditions on the volume fraction of Goss texture at the position 0.4 mm below the surface

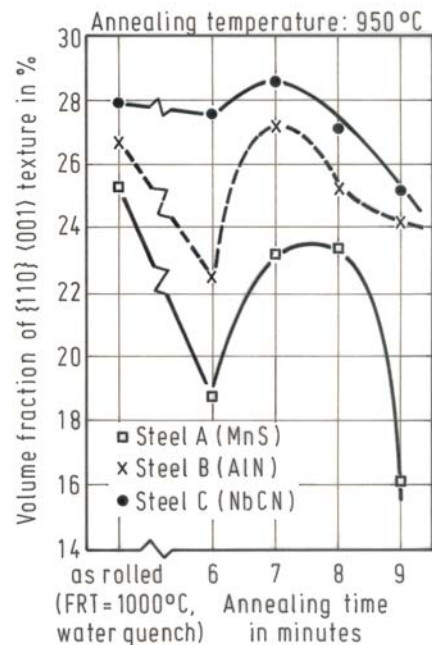


Figure 5: Influence of hot band annealing on the volume fraction of Goss texture at position 0.4 mm below the surface

Annealing samples with the highest volume fraction of Goss texture (FRT = 1000°C, water quench) at 950°C for several minutes, only marginal effected the volume fraction of texture components compared to the as rolled condition, **Figure 5**. These results indicate that the 'normalising' treatment could be avoided for material with optimized hot rolling conditions.

Cold rolled sheet. The change in the microstructure, which occurred after the first cold rolling step and the various annealing conditions was investigated at the mid thickness position and is summarized as follows:

The grain size increased exponentially with higher annealing temperature and longer annealing time, as shown in **Figure 6**. This was especially evident with the 'MnS' steel A, while in steel B and C no remarkable grain growth occurred at 920 °C even after 1.5 hours, confirming that AlN and Nb(C,N) are very effective in controlling the grain size.

In all three cold rolled and annealed steels the volume fraction of Goss texture was higher than in the hot strip material. It also increased with longer annealing time and in most cases was higher with a higher annealing temperature. However, for the longest annealing time and the highest annealing temperature tested in this study, not necessarily the highest volume fraction of Goss texture was obtained, **Figure 7**. Comparing equal annealing conditions, the 'MnS' steel A showed the weakest and the Nb(C,N) steel C the strongest $\{110\}<001>$ orientation.

Samples, recrystallized annealed at 920°C for five minutes were further cold rolled by 50%. Then the second primary recrystallization plus decarburization heat treatment and finally the secondary recrystallization annealing were carried out. **Figure 8** shows that the absolute value of Goss texture exhibited more than double the volume fraction

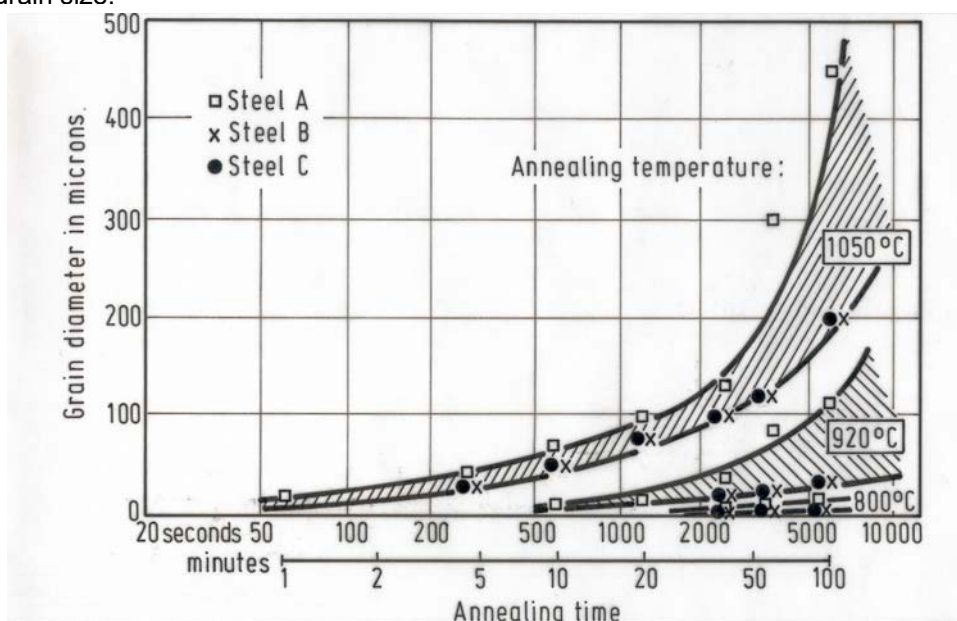


Figure 6: Grain size after the 1st recrystallisation annealing

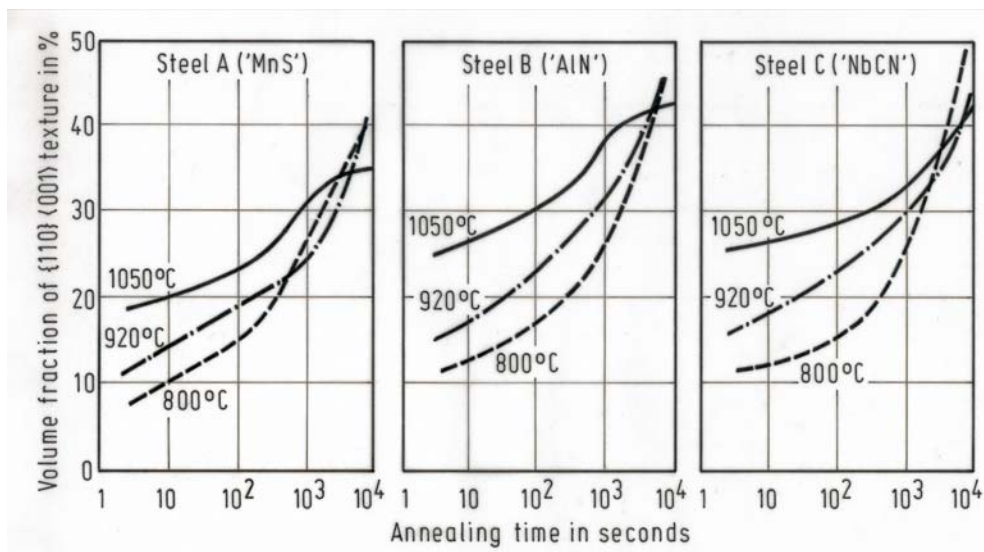


Figure 7: Volume fraction of Goss texture after the 1st recrystallisation annealing

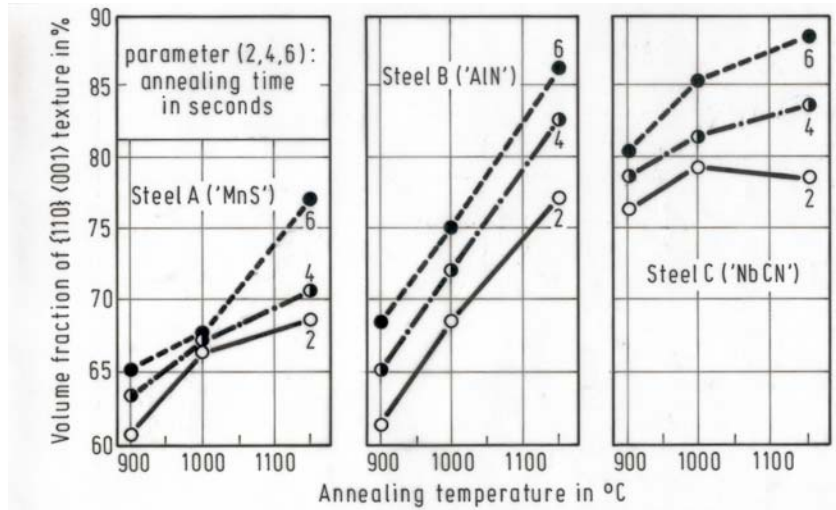


Figure 8: Goss texture development during secondary recrystallisation

compared to the observation after the first recrystallization treatment. Furthermore, the Goss orientation increased with higher annealing temperature and longer annealing time and the ranking of the three steels became more pronounced. Steel C, based on Nb(C,N) as inhibitor phase showed a {110}<001> volume fraction of more than 75% already at the lowest annealing condition tested, i.e. at 900°C for two hours, and also exhibited the highest value with 88.5%. On the other hand the second best steel B, based on the AlN technology required an annealing temperature of 1150°C to obtain more than 75 volume percent of Goss texture. This is a clear indication of the effective role of Nb(C,N) in controlling the grain size during the first recrystallization has been drastically reduced after decarburization, allowing the Goss texture to grow easily. On the other hand the dissolution of AlN particles obviously needs higher temperatures than necessary for Nb(CN) and thus is in agreement with the solubility products. These results confirm that both the Goss and the cube texture, which are present already in the hot rolled material, are stable orientations and were not reduced during cold rolling and primary recrystallisation and the {111}<112> orientation rotates during the secondary recrystallisation to the desired {110}<001> texture component [23,24]. **Figure 9** illustrates that the second cold rolling reduction of 50% is an optimized condition for the Nb(C,N) and the AlN steels, while for the MnS variant a higher cold rolling degree seems to be needed to achieve a high Goss texture orientation.

Compared to the results obtained with the two steps rolling trials a much lower volume fraction of Goss texture is observed, when a single-stage rolling schedule is applied to achieve the same final sheet thickness. Furthermore, a higher total cold rolling reduction than 80% does not help to achieve better data, **Figure 10**. These findings underline the importance of the primary recrystallization after a first cold rolling deformation within a two-steps rolling reported published data [25,26].

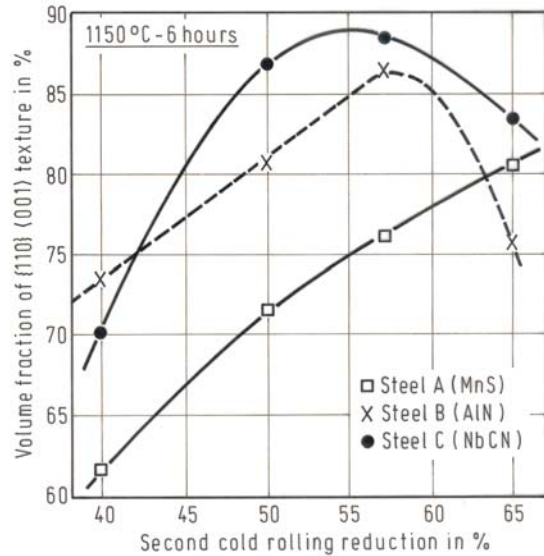


Figure 9: Influence of second cold rolling reduction on Goss texture development

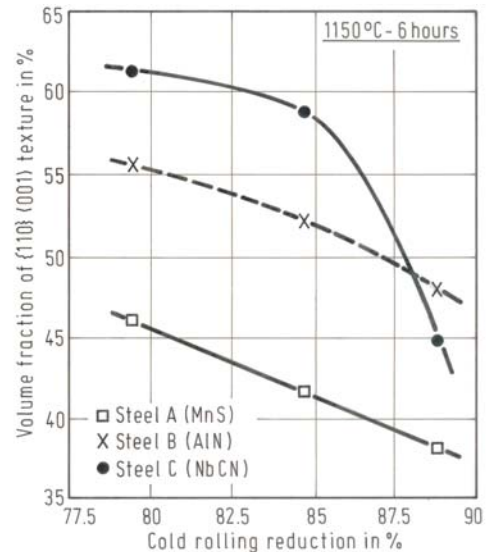


Figure 10: Goss texture development after single stage cold rolling deformation

Core losses. The results of measurements obtained with 'transformer sheets' of laboratory trials were compared with industrial production data in **Figure 11**. It is obvious that the results from these trials were inferior to standard production, which relied on a slightly higher annealing temperature for secondary recrystallization of 1175°C. However, there are at least two more reasons for this deterioration: Firstly, the laboratory processing route with regard to total deformation, deformation speed, etc. was not identical to an industrial rolling schedule. Therefore the results achieved with laboratory processing of the industrially melted slab sample A were not equal to those from industrial production; and generally inferior. Secondly, the laboratory heats of steel B and C exhibited a much poorer cleanliness than the industrially produced heat A, causing samples from steel A to exhibit equal or better core losses than the samples from steel B, which comprised a more favorable crystallographic texture. The argument for poor cleanliness also applies for steel C with Nb(C,N) as the inhibitor phase. Despite this deficit, and especially when just the laboratory studies were compared, this alloy design resulted in the lowest core losses.

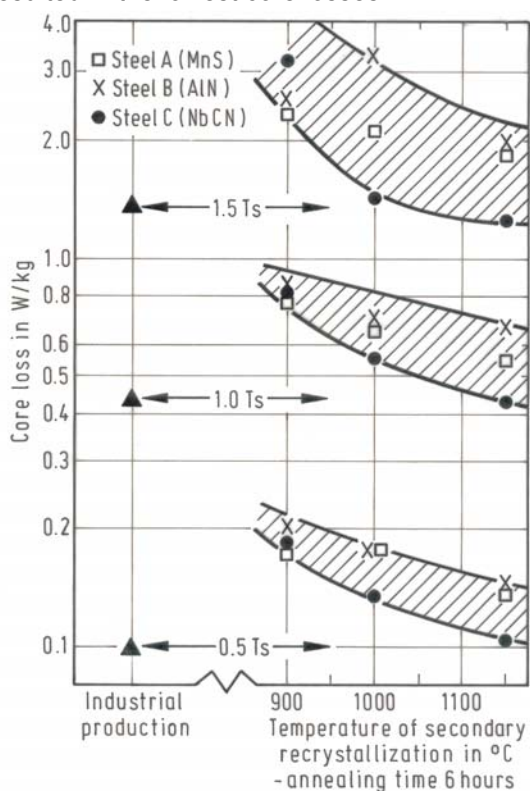


Figure 11 :Core losses of laboratory trials compared to industrial production

Summary and conclusions

From solubility product considerations, Nb(C,N) could be a suitable inhibitor phase. The characteristic features of an inhibitor phase are the control the grain size during the first and second primary recrystallization and permitting the formation of a

high volume fraction of Goss texture during the secondary recrystallization annealing.

Since niobium also forms carbides, this element might add to aging stability of the final product, which is not possible by other elements that are typically applied.

It was found, that the niobium microalloyed silicon steel already exhibited after hot rolling the highest volume fraction of the favorable Goss texture at a position of 0.3 to 0.4mm below the strip surface. With a faster cooling rate, this texture component was higher and an additional heat treatment of the hot rolled material may not be required to achieve further improvement.

The relatively high volume fraction of Goss texture observed in the hot rolled material of the Nb(C,N) variant persisted after all the various cold rolling and annealing steps. It grew to volume fractions above 40% after the first cold rolling step plus intermediary primary recrystallization and to more than 80% after the second cold rolling step, the decarburization plus secondary recrystallization anneal.

A two stages cold rolling schedule with an intermediary recrystallisation treatment was necessary to obtain a sharp Goss texture. In this case a higher annealing temperature and longer holding time during the secondary recrystallization were favorable for Goss texture maximization and the Nb(C,N) variant again gave the best results. Furthermore, the dissolution kinetics of this inhibitor phase opened the possibility to obtain the desired texture already at lower annealing temperatures.

Consistent with the highest volume fraction of Goss texture, the core losses were lowest with the Nb(C,N) inhibitor phase compared to variants with AlN or MnS.

Silicon steel processed via a single stage rolling schedule and total a deformation being not higher than 80% will also exhibit relatively low core losses when using niobium microalloying, as result of the already high level of Goss texture component obtained after the hot rolling operation. It is proposed, that this concept might be applicable for the production of dynamo electrical sheet.

The relatively high volume fraction of Goss texture already existing in the hot rolled material and the effective behavior as inhibitor phase makes niobium an interesting alloy for optimizing grain oriented electrical sheet. Confirmation of these laboratory results in industrial production is foreseen.

Acknowledgement

This study was carried out in the framework of the doctoral thesis of Mrs. Ana Doniga. Mrs. Doniga is especially grateful to Prof. A. Dumitrescu of the institute ICEM in Bucharest for stimulating discussions and guidance during the research work. Thanks are also expressed to the Romanian companies Sidex in Galati and COST in Tirgoviste for production and fabrication of the laboratory

samples and to ICEM for support of the material testing.

References

- [1] Werkstoffkunde Stahl, Verlag Stahleisen, Düsseldorf (Germany), 1984, Volume 1, Chapter C2 (Physical properties), p. 401
- [2] Werkstoffkunde Stahl, Verlag Stahleisen, Düsseldorf (Germany), 1984, Volume 2, Chapter D 20.4 Electrical sheet, p. 501
- [3] N.P. Goss, US patent 1 965 559, 1934
- [4] C.M. Vlad, unpublished report on 'Texture Control of Electrical Sheet', Stahlwerke Peine-Salzgitter AG, Salzgitter (Germany), 1976
- [5] W. C. Leslie et al., Trans. Am. Soc. Met, 53 (1961), p. 715
- [6] W. C. Leslie, The Physical Metallurgy of Steels, Hemisphere Publishing Corporation, Washington (US), 1981, Chapter 11, p. 318
- [7] J.E. May and D. Turnbull, Trans. of TMS of AIME, Vol. 212, Dec. 1958, p. 769
- [8] J. Harase et al., Trans. ISIJ, Vol. 27, 1987, p. 965
- [9] J. Kunze, Nitrogen and Carbon in Iron and Steels—Thermodynamics, Akademie Verlag, Berlin (Germany), 1991, p. 192
- [10] R.W. Fountain and J. Chipman, Trans. Met. Soc. AIME 224 (1962), p. 599
- [11] J. Kunze and J. Reichert, Neue Hütte 26 (1981), p. 23
- [12] W. Roberts and A. Sandberg, Swed. Inst. for Met. Res. Report IM 1489, Stockholm (Sweden), 1990
- [13] B.S. Ivanov et al., Stal, 1996, No. 8, p. 52
- [14] H.C. Fiedler, Met. Trans. 9A (1978), p. 1489
- [15] A.H. Wriedt, Met. Trans. 11A (1980), p. 1731
- [16] A.H. Wriedt and H. Hu, Met. Trans. 7A (1976), p. 711
- [17] G. Parvu, V. Miron and C. Winckelbauer, Journal of Magnetism and Magnetic Materials 112 (1992), p. 169
- [18] R.D.Cullity, Elements of X-ray Diffraction, Addison-Wesley Press, 1956, p.290
- [19] C.M.Vlad, unpublished report on 'Inverse Pole Figure Method', Stahlwerke Peine-Salzgitter AG, Salzgitter (Germany), 1972
- [20] E.Hug and F.Dumas, Revue de Metallurgie, 1994, Vol.12, p.1857
- [21] V.Ya.Goldhein, Fiz. Met. Metalloved, 1980, Vol.50, p.1213
- [22] A. Doniga, C.M. Vlad and K. Hulka, Metallurgy and New Materials Researches, Vol. VIII, No. 4/2000, p. 29
- [23] H. Hu :Trans.AIME,vol.221, 1961, p.130
- [24] D.M.Kohler and M.F.Littmann: U.S.Patent 3130094
- [25] H.C. Fiedler, G.E. Report No 64.RL-3842M, Recrystallisation Textures, 1964
- [26] H.E. Grenoble, US patent 3905842, 1975

Klaus Hulka, Niobium Products Company GmbH, Düsseldorf; Germany, Dr. Constantin M. Vlad, Consultant, Rülzheim, Germany, Dr. Ana Doniga, University Dunarea de Jos, Galati, Romania.